

Date of publication xxxx 00, 0000, date of current version xxxx 00, 0000.

Digital Object Identifier 10.1109/ACCESS.2017.Doi Number

# Detection of Wheat Unsound Kernels Based on Improved ResNet

Hui Gao, Tong Zhen, and Zhihui Li

College of Information Science and Engineering, Henan University of Technology, Zhengzhou 450001, China  
Key Laboratory of Grain Information Processing and Control, Ministry of Education, Henan University of Technology, Zhengzhou 450001, China

Corresponding author: Zhihui Li(e-mail:653081735@qq.com).

This work was supported by the National Key Research and Development Project under Project 2018YFD0401404.

**ABSTRACT** In the process of grain acquisition, the unsound kernel of wheat is detected mainly by manual detection, and the method of detection by computer vision is still in the experimental stage. Aiming at the problems such as expensive equipment for image acquisition, difficulty in adhesion segmentation, and low recognition efficiency in detection, this paper takes six kinds of wheat as objects, namely sound kernel, broken kernel, sprouted kernel, injured kernel, moldy kernel and spotted kernel, builds a wheat image acquisition platform, and establishes a two-kernels adhesion wheat segmentation algorithm based on concave-mask. Among the total 9988 wheat grains, the error rate accounts for 0.93%. By comparing the advantages and disadvantages of GoogleNet, DenseNet, IX-ResNet, Res2Net, exploring the improvement of depth, width, downsampling mode, convolution order, attention mechanism18, receptive field, and finally puts forward a wheat unsound kernel detection model based on Res24\_D\_CBAM\_Atrous. The Macro avg values of Precision, Recall and F1 are 94%, 95% and 94%, respectively, which are increased by 3%-4% based on the original Res34 and the prediction time is reduced by 220s, which can meet the rapid and accurate evaluation of wheat appearance quality, and has important theoretical significance and practical application value for wheat market circulation.

**INDEX TERMS** Unsound kernels, Image acquisition platform, Adhesive segmentation, Improved ResNet, Classification.

## I. INTRODUCTION

In 2021, the sown area of wheat is about 23 million hectares and the output reaches 134 million tons, accounting for about 20% of the sown area and output of grains in China, so the quality of wheat is directly related to the national economy and people's livelihood [1]. Unsound kernel refers to damaged wheat kernels that are still valuable, including injured kernel, spotted kernel (gibberella damaged kernel and black germ kernel), broken kernel, sprouted kernel and moldy kernel. The appearance features are as follows: Injured kernels have many insect-eroded holes on the surface; Gibberella damaged kernels are shriveled and stiff-white, the kernel surface is purple or accompanied by pink mildew; The embryo surface of black germ kernels is dark brown or black; Broken kernels are flattened and broken; Sprouted kernels show the seed coat of the embryo broken, obviously bulged or the bud and radicle breaks through the seed coat, The main effects are as follows: the changes of starch physicochemical properties, protein content, gluten structure and uric acid content, resulting in peculiar smell, darkening

color, pollution and quality deterioration of processed products [2], [3]; Even the continuous accumulation of mycotoxins seriously endangers the health of humans and animals [4], [5]; The increase of sprouted kernels and moldy kernels leads to the decrease of wheat test weight [6]; In the process of wheat acquisition and circulation, the unsound kernel is used as the limiting index of quality and as the basis for increasing or deducting amount [7]. To sum up, the detection of wheat unsound kernels is of great significance to the evaluation of wheat quality.

At present, the detection of wheat unsound kernels mainly exists in grain depots, processing factories and quality inspection department, and the technology mainly stays in manual detection. The deviation and fatigue in the understanding of unsound kernels is easy to cause grading errors; There is a risk of collusion and fraud among inspectors; The low detection efficiency will directly affect the acquisition progress of the whole batch of grain [8], [9]. Hyperspectral imaging technology has the advantages of machine vision and spectral analysis, but the problem of large amount of data and expensive system cannot be avoided [10]. Acoustical detection technology can detect

injured kernels according to different signals generated by wheat hitting metal targets, but it is easily interfered by noise [11]. Micro X-ray CT technology can observe the surface characteristics and internal structure of wheat kernels in an all-round way, but it is necessary to find a more effective three-dimensional reconstruction method [12]. Traditional machine learning method can capture crop images through computer vision system, extract features according to color, shape, area and texture [13]. However, manual feature extraction relies on human prior knowledge, and the features are interrelated, resulting in redundancy, which can no longer meet rapid and accurate evaluation of appearance quality [14].

So, the application of deep learning in the field of grain inspection has been widely concerned. In the detection of corn kernels, Huang *et al.* [15] first adopted VGG19 transfer learning, and the result was better than the traditional machine learning algorithm, but the accuracy was still not ideal. Then they adopted more complex GoogLeNet, the recognition accuracy rate reached 96.5%; Zhao *et al.* [16] used electromagnetic vibration platform to arrange corn kernels in batches, and built a visual classification system based on Faster R-CNN to achieve better recognition, and pointed out that the smaller and faster model, double-sided detection of corn kernels need to be further studied; Ni *et al.* [17] designed a double-sided corn automatic detector, which separated two adhesive kernels based on K-means clustering of curvature, and embedded ResNet into corn grain evaluation system, and the prediction accuracy of 408 test images reached 98.2%; Altuntas *et al.* [18] identified haploid and diploid maize seeds through transfer learning, and compared with AlexNet, VGGNet, GoogleNet and ResNet, obtained the most effective VGG-19, and realized rapid and low-cost classification. In the detection of rice, Kiratiratanapruk *et al.* [19] compared VGG16, Xception, Inception V3 and InceptionResNet V2, and found that the classification accuracy of InceptionResNet V2 was the highest. At the same time, it was found that appropriate reduction of image size and redirection of rice seeds can improve the detection effect. To distinguish falsely marked rice, Gilanie *et al.* [20] designed an 18-layer CNN rice classification model, which had better classification effect than VGG19, ResNet50 and GoogleNet. In the detection of wheat unsound kernels, ZHANG *et al.* [21] constructed the ResNet50 by adding attention mechanism to the residual networks (18, 34, 50, 101) of different depths, and the average recognition rate of 6 types of wheat kernels reached 96.5%; Zhang [22] constructed a ResNet with only three blocks, added a pooling with step size of 2 between residual blocks, made the downsampling independent, and added a 5×5 convolution layer to ensure that the input and output have the same number of channels, instead of the dotted connection, the recognition accuracy of 7 types of wheat kernels reached 96.3%. Zhu *et al.* [23] collected sound and broken kernels, compared LeNet-5, AlexNet, VGG-16 and

ResNet, established a wheat sound kernels detection system based on AlexNet with an average recognition rate of 96.67%. Therefore, the grain crop recognition method based on deep learning has become the mainstream algorithm.

In practice, the detection of wheat unsound kernels based on deep learning is rare. The main reason is not only that the classification network of wheat unsound kernels still stays in a simple classification model, but also that the image acquisition equipments and segmentation methods seriously restrict recognition efficiency. The mainstream image acquisition methods are divided into: the ways of grains oscillating and falling [24], fixing a single kernel in an independent hole [22]-[25], oscillating, separating the grains and scanning them linearly [16]. It can be seen that more unsound kernels detection relies on equipment, which reduces the difficulty of segmentation, but requires higher equipment accuracy and hardware cost. In addition, some scholars abandoned the research of equipment, and placed grains on the image acquisition platform one by one manually, or tended to identify single kind of grains, completely divorced from the adhesion and randomness of grains in actual scenes [21]-[23]. To sum up, combining the dual advantages of equipment and segmentation method, a fast and accurate multi-grain detection model is established, which provides a scientific basis for the quality evaluation in wheat market circulation.

## II. MATERIALS AND METHODS

### A. IMAGE ACQUISITION PLATFORM

In this study, a simple wheat image acquisition platform was built, as shown in Fig. 1. The platform included industrial camera bracket, electromagnetic vibration table, tray, light source, industrial camera. The 900mm industrial camera bracket is fixed on the lab bench, and the bottom is placed with a small electromagnetic vibration table, model HTA-3000A, with a frequency of 50Hz and vertical vibration, with a size of 350 × 400 × 250mm, controlling the vibration frequency and promoting the uniform distribution of wheat kernels; A black tray is fixed above the vibrating table with a size of 350×350mm, which is made of non-reflective melamine to reduce the interference of background; The light source is erected above the tray, 16 led light bars with length of 40cm and 48w are selected and combined into a square light source with 8 horizontal and 8 vertical beams, and a square hole is left in the middle to ensure that the visual field of the camera is not obstructed and the image background is uniform while providing sufficient brightness; Next to the light source, Hikvision industrial camera, model MV-CE100-30GC, 10 million pixels, supporting MVS software, can adjust the image detail information, and can clearly present the characteristics of wheat color and shape; Finally, brush is used to clear the wheat kernels outside the visual field around the edge of the tray to prevent the incomplete grains from affecting the recognition result.

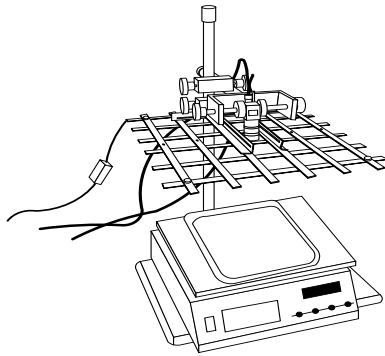


FIGURE 1. Wheat image acquisition platform.

### B. IMAGE ACQUISITION

The wheat samples were provided by Xinglong National Grain Reserve in Zhengzhou, Henan Province, including unsound kernel, broken kernel, sprouted kernel, injured kernel, moldy kernel and spotted kernel (the spotted kernel is

mainly black germ kernel), which were screened by professional quality inspectors. The wheat kernels were about 210g, which were fully mixed. 50g of mixed samples were randomly weighed as test set samples, and the remaining 160g were taken as training set samples. Take about 5g of the mixed sample of 160g each time, put it on the tray, turn on the vibrating table to make the samples uniformly distributed, and then collect the images. After the first round of collection, repeat the above operations, and finally collect 100 mixed images. In order to fully mine the characteristics of wheat, manually classify the mixed samples, and take 5 images of each wheat sample, with a total of 130 images as the original images for establishing the training set. 50g mixed samples, using the same operation as above, a total of 13 mixed type images are obtained as the original images for establishing the test set. original images of wheat mixed kernels are shown in Fig 2.



FIGURE 2. Original images of wheat mixed kernels

### C. IMAGE SEGMENTATION

In deep learning, the detection of wheat unsound kernels is based on single kernel recognition, so the original image must be single-grained. It can be seen from Fig. 2 that the adhesive kernels inevitably still exist widely, but the number of adhesive kernels and the segmentation difficulty have been greatly reduced. On this basis, we need to combine the segmentation algorithm for further processing.

In the task of classification, counting of agricultural products such as wheat and corn, it is often necessary to combine the adhesion segmentation algorithm. The single segmentation method based on threshold, edge detection, region, clustering, morphology and active contour, can not completely segment the adhesive kernels, but often serve as an intermediate means and a preprocessing method [26]. The segmentation method based on watershed is affected by image noise, local irregularities and subtle gray changes on the grain surface, will form a minimum value in the interior, resulting in over-segmentation [27]. Concave-based segmentation methods are generally summarized as three

steps: concave detection, concave matching and concave segmentation. Concave detection often uses curvature, angle, convex hull, chain code, template search and to obtain the location of concave, and then realizes segmentation through concave matching, directional corrosion, circle fitting, which is extremely suitable for the segmentation of adhesion kernels [28], [29].

On the basis of the original image, the segmentation algorithm of adhesive wheat with two-kernels based on concave-mask is adopted.

The first part is image preprocessing. The original image is gray-processed, and in order to eliminate the low-frequency noise in the image, the bilateral filtering method is adopted to highlight the edge and texture characteristics of wheat; Because of the large field of view, it is difficult to illuminate the light evenly, and the ideal segmentation effect can not be achieved only by fixed threshold, so the adaptive threshold method is used for binarization; The binary image is edge smoothed by morphological open-close operation to separate wheat targets from the background.

The second part is the segmentation of adhesive kernels. By setting the threshold of wheat area, two or more adhesion kernels were screened out; Because the shape of wheat kernels is elliptical, and the shape of defect area formed between adhered kernels is simple, the convex hull method is selected to determine the concave position. As shown in Fig. 3, the area of adhered wheat is enlarged and displayed. The convex hull location is the smallest circumscribed polygon

area of adhered wheat, which is surrounded by green line, and the contour of adhesive wheat is surrounded by blue line. Subtracting convex hull area from the contour area of adhesive wheat, which is the defect area. By judging the number of defects in the area, extract the two parts with the largest defect area, determine the concave position, and connect the two parts with red line to realize the segmentation of two adhesive kernels.

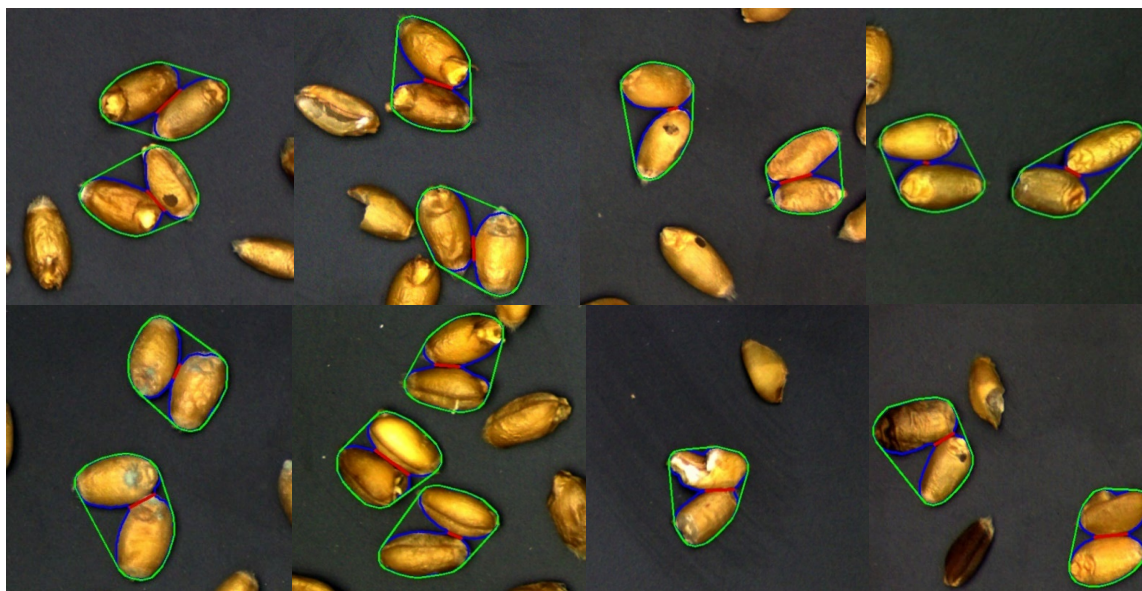


**FIGURE 3.** Segmentation images of adhesive wheat kernels

The third part is cropping single kernel wheat image. The single kernel wheat images without adhesion or after adhesion segmentation are mainly used as the mask images, and the wheat in the original image can be segmented

through mask processing. Then, the best angle, height and width of wheat segmentation are found by rotating the smallest external rectangle. Finally, the wheat images are cropped into many single kernel images. As shown in Fig. 4.

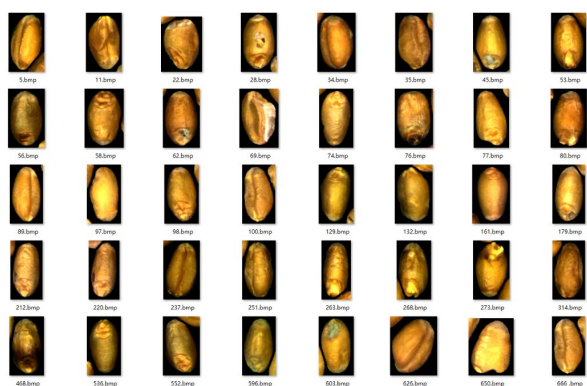


**FIGURE 4.** Cropped single-kernel image

The fourth part is to abandon the redundant contour. It can be seen from Fig. 5 that the cropped single-kernel wheat images have more or less redundant parts, mainly because the wheat is close to each other, and the minimum rectangular cropping method cannot completely avoid neighboring wheat. The main method is to extract the largest

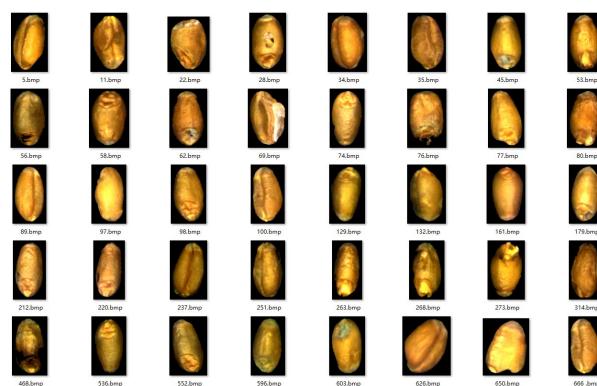


**FIGURE 5.** Single-kernel image without redundant contour

contour from the binary image as a mask, discard the redundant contour, mask the cropped single-kernel wheat image and save them. As shown in Fig. 6.

By cropping and segmenting 130 original images, the segmentation results of various wheat kernels are shown in Table 1.

TABLE 1. Wheat Kernels Image Segmentation Results

Category	Number of effective segmentation	Number of false segmentation	Rate of false segmentation	Reason of false segmentation
Sound	2827			
Sprouted	1422			
Injured	1193	93	0.93%	Circular adhesion of multi-sprouted; The area of two adhered-injured is less than that of single-sound; Error in concave detection of single-damaged; The black spots of spotted are lost after binarization.
Moldly	1606			
Broken	1778			
Spotted	1069			

To sum up, based on the image acquisition platform, combined with the segmentation method of adhesive wheat with two-kernels based on concave-mask, the error segmentation rate is 0.93% in a total of 9988 wheat images, and the effect is better.

#### D. MAKING DATA SETS

For all kinds of wheat kernels, 800 kernels are randomly selected for each kind, totaling 4800 kernels of wheat. In order to prevent network over-fitting, improve generalization ability, and apply to more scenes, the image is enhanced by three ways: increasing brightness after rotating 180, adding noise, and reducing brightness after mirroring [30], and each type of wheat image is expanded to 3200, totaling 19200 wheat images. The data sets were divided according to the ratio of training set to verification set of 8:2. A total of 15360 training set images and 3840 verification set images were obtained. Through the above segmentation method, 13 original images collected from 50g mixed wheat samples were segmented and cropped, and 1113 wheat images were obtained as test sets.

### III. DEEP LEARNING MODELS

#### A. MODELS AND METHODS

In this paper, the typical GoogleNet, ResNet, DenseNet and ShuffleNet models are compared, and the advantages and disadvantages of their respective network frameworks are combined to improve the ResNet, and finally the optimal model for wheat unsound kernels detection is obtained.

The advantage of GoogleNet lies in the proposal of Inception module, which greatly increases the number of network channels, and uses sparse connection to separate channels, increase the network width and reduce the number of parameters; In order to increase the receptive field, a large-size convolution kernel is used; Convolution kernels of 1×1, 3×3, and 5×5 are used for dense connection to fuse multi-scale information. The disadvantage of this network is that the Inception module is limited to high-level applications, the underlying structure remains traditional [31].

The advantage of ResNet lies in the proposal of residual module, which mainly builds deep network by stacking different residual blocks, and extracts abundant features; Skip

connection is adopted to avoid the problem of network degradation caused by too deep network, and 1×1 convolution is added to realize channel dimension reduction; BN is introduced to accelerate the training. The main disadvantage is its limited ability to capture multi-scale features, its downsampling with step size of 2 and 1×1 convolution to result in the loss of feature information and long training time [32].

The advantage of DenseNet lies in the proposal of dense connection, and the multiple concatenations in dense block make the best use of the feature map, which makes the accuracy comparable to ResNet; The 1×1 convolution guarantee network in transition layer is narrow, and the sequence structure of BN, Relu and Conv greatly reduces the parameter quantity. The main disadvantage is that the dense connection may bring redundancy, and the video memory is too large [33].

The advantage of ShuffleNet lies in the proposal of Channel shuffle, which reduces the amount of computation and enriches feature learning; Using 1×1 group convolution, 3×3 depth separable convolution to replace the original convolution, using concatenation to replace the original add, greatly reduce the amount of parameters; The average pooling of 3×3 convolution and step size 2 is used to replace the downsampling to increase the feature transfer. The guiding principle of ShuffleNet V2 indicates that the number of input and output channels must be balanced, the degree of network fragmentation and the use of relu and add should be reduced [34].

Park *et al.* [35] combined attention mechanism SENet with ResNet, and added SE to different depth layers of ResNet (18/34/50/101/152), which was suitable for 7 classification of electrocardiogram signals. Miao *et al.* [36] based on ResNet29, introduced gating strategy into residual unit, which changed feature fusion from adding the same weight to weighted summation, and pointed out that the performance improvement brought by gating strategy decreased with the increase of network complexity. Tao *et al.* [37] proposed a fragmented multi-scale feature fusion network IX-ResNet with reference to the Inception, which used 1×1, 3×3, 5×5 group convolution to fuse multi-scale information, and improved the performance with 1×3, 3×1, 1×5, 5×1 convolution. The Res2Net proposed by Gao *et al.* [38] inserted more hierarchical residual connection structures into

the residual unit, increased the receptive field, and realized feature fusion at a finer granularity level. Lu *et al.* [39] proposed a ResNet embedded with pyramid-shaped atrous convolution, and used atrous convolution with rates of 1, 3 and 5 in the bottom residual block to fuse multi-scale information and improve classification performance. Woo *et al.* [40] added SE and CBAM to each residual block of ResNe18, ResNet34, ResNet50, ResNt101, and the comparison shows the model with CBAM higher accuracy.

### B . MODELS OPTIMIZATION

Obviously, the model is optimized mainly by changing depth and width, multi-scale feature fusion, adding attention mechanism, changing topological structure, optimizing training parameters.

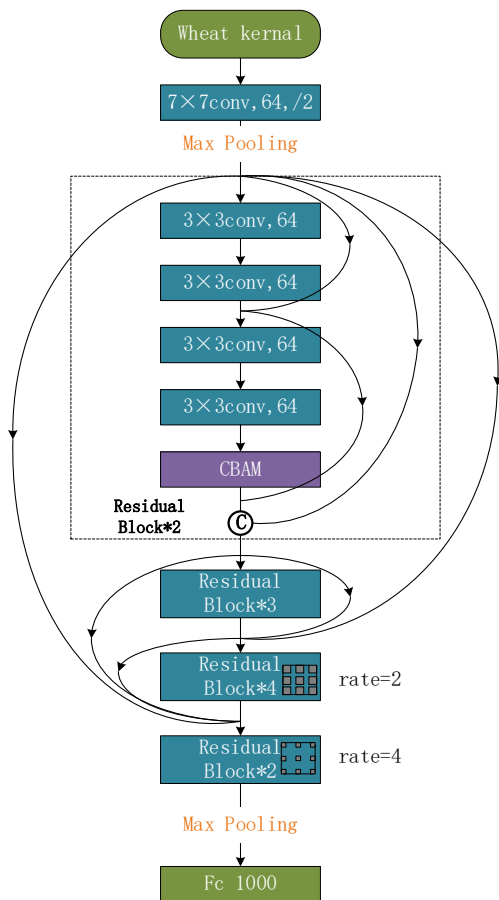


FIGURE 6. Res24\_D\_CBAM\_Atrous model

For the depth of network, considering that the wheat unsound kernel have few types and simple features. There is redundancy in feature extraction of ResNet, so a 24-layer ResNet is designed. The number of residual modules is 2, 3, 4 and 2, respectively, named Res24; In terms of width, dense connection is introduced into the first three layers, and the concatenation is used to splice the outputs of each layer with ones of dense connection. Because the number of output channels of each layer is consistent with input channels of the

next layer, the dashed line of skip connection does not need upgrade dimension by  $1 \times 1$  convolution, instead, it is replaced by the average pooling with convolution kernel of  $3 \times 3$  and step of 2, and the sequence of Conv, BN and Relu is changed to BN, Relu, Conv, named Res24\_D; Considering the small characteristics of unsound kernels, CBAM is added to the last Block of each layer, named RES 24\_D\_CBAM; At last, the atrous convolutions with rates of 2 and 4 are added to the block in the third and fourth layers, and the step of the fourth layer is set to 1, and the receptive field of  $7 \times 7$  is converted to  $14 \times 14$ , named Res24\_D\_CBAM\_Atrous. The main frame diagram of the improved Res24\_D\_CBAM\_Atrous is shown in Fig. 6.

## IV. RESULTS

### A . MODELS AND METHODS

The experimental software and equipment configuration parameters are as follows: Intel (R) Xeon (R) E5-2620 V3 2.40GHz, two NVIDIA Telsa T4 GPU, two 16GB RAM, Ubuntu 18.04, pytorch1.7.1, Python3.6.13 and CUDA10.0.

### B . EVALUATION INDEX

The evaluation indexes selected in this experiment are as follows: in the training process, the accuracy of the current model is expressed by Accuracy; The Loss function curve indicates the difference between the predicted and the actual. In the test set, Precision indicates the proportion of correctly predicted positive samples to actually predicted positive samples. The Recall rate indicates the proportion of correctly predicted positive samples to actual positive samples. F1 value shows the harmonic average of precision and recall rate; Macro avg represents the arithmetic average of performance indicators of each category; Support is the number of times the real label appears; Confusion Matrix can directly display the final classification results of the model. Time means the prediction time for the same batch of unsound kernels under the same conditions.

$$Precision = \frac{TP}{TP + FP} \quad (1)$$

$$Recall = \frac{TP}{TP + FN} \quad (2)$$

$$F1 = 2 \cdot \frac{Precision \cdot Recall}{Precision + Recall} \quad (3)$$

where TP (True Positive) stands for correctly predicting positive samples as positive, FP (False Positive) stands for incorrectly predicting negative samples as positive, TN (True Negative) stands for correctly predicting negative samples as positive, and FN (False Negative) stands for incorrectly predicting positive samples as negative.

### C . MODELS AND METHODS

In this experiment, by comparing six models, such as Res18, Res34, Res24, Res24\_D, Res24\_D\_CBAM, Res24\_D\_CBAM\_Atrous, during training, the image size is

uniformly scaled to 224×224, the batch size is 16, the number of iterations is 30, and the learning rate is 0.001. The training results is shown in Figure 7.

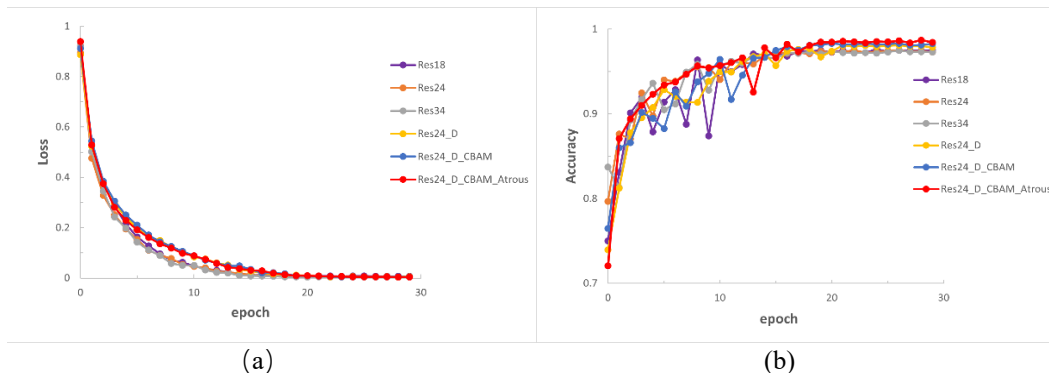


FIGURE 7. Training results:(a)Training loss;(b) Verification accuracy

As can be seen from Fig. 7, for the Res18, Res24 and Res34 models, the convergence speed of the training loss function is roughly the same and slightly faster than the other three improved models, but in the verification set, the accuracy is significantly lower than the three improved models. Among the iterations of different epochs, the accuracy of Res18 and res34 models is the lowest, even the accuracy of Res18 is extremely unstable, while the accuracy of Res24 fluctuates very little, and it shows the same

accuracy as Res34 in shallow network depth. In the three improved models, Res24\_D, Res24\_D\_CBAM and Res24\_D\_CBAM\_Atrous, the convergence speed of loss function decreases slightly with the increase of the model complexity, but the accuracy increases with continuous optimization, and the Res24\_D\_CBAM\_Atrous model performs best.

In the test set, the classification evaluation indexes of different ResNet are shown in Table 2.

TABLE 2. Classification performance evaluation of different ResNet

Model	Accuracy	Precision	Recall	F1	Time(s)
Res34	0.91	0.91	0.91	0.91	698
Res18	0.90	0.90	0.92	0.91	437
Res24	0.92	0.91	0.93	0.92	451
Res24_D	0.92	0.92	0.93	0.93	486
Res24_D_CBAM	0.93	0.93	0.94	0.93	453
Res24 D CBAM Atrous	0.94	0.94	0.95	0.94	478

Based on more feature extraction layers, the performance of Res34 is slightly higher than that of Res34, but the classification time is greatly improved, which means that Res34 has redundancy. Therefore, the Res24 is selected for improvement. After three times of optimization, the average index Accuracy, Precision, Recall and F1 of wheat classification reaches 94%, 94%, 95% and 94%, respectively,

which is increased by 3%-4% based on Res34. The prediction time is reduced by 220s, which indicates that the proposed Res24\_D\_CBAM\_Atrous has better generalization ability and greatly improves the overall performance.

Classification performance evaluation and confusion matrix of various wheat based on Res24\_D\_CBAM\_Atrous are shown in Table 3 and Fig. 8.

TABLE 3. Classification performance evaluation based on Res24\_D\_CBAM\_Atrous

Category	Precision	Recall	F1	Support	Time(s)
Broken	0.93	0.98	0.95	206	478
Injured	0.95	0.95	0.95	149	
Moldy	0.96	0.95	0.96	126	
Sound	0.94	0.92	0.93	390	
Spotted	0.89	0.95	0.92	94	
Sprouted	0.97	0.93	0.95	148	

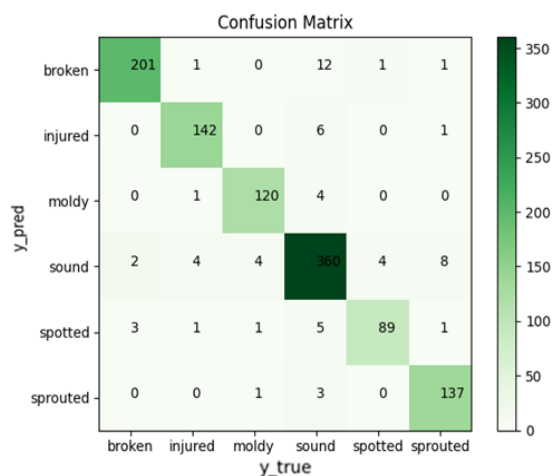


FIGURE 8. Classification confusion matrix based on Res24\_D\_CBAM\_Atrous

To sum up, in the test set of 1113 wheat kernels, the improved Res24\_D\_CBAM\_Atrous shows that the F1 values of all kinds of wheat are above 92%, and the F1 values of moldy kernels are the highest, reaching 96%. For the actual 206 broken kernels, 201 kernels are correctly detected, and only 5 broken kernels are misjudged as sound kernels and spotted kernels, but the predicted broken kernels reach 216, resulting in recall value greater than precision value; For the actual 149 injured kernels, 142 kernels are correctly detected. The main error source is that some insect-eroded holes of injured kernels are located at the edge of wheat, which is difficult to distinguish and misjudged as sound kernels, but the same number of other kinds of wheat are misjudged as

injured kernels, resulting in the same recall value and precision value. For the actual 126 moldy kernels, 120 kernels are correctly detected. The main error source is that the area of moldy parts is small and confused with sound kernels, resulting in similar precision value and recall value. For the actual 390 sound kernels, 360 kernels are correctly predicted, 12 sound kernels have small area, which are misjudged as broken kernels, 6 sound kernels have spots, irregular contours on the surface, which are misjudged as injured kernels, 4 sound kernels' top hairs are misjudged as moldy, 5 sound kernels have black spots, which are misjudged as spotted kernels, and 3 sound kernels have irregular bulges on the embryo, which are misjudged as sprouted kernels. For the actual 94 spotted kernels, 89 kernels are correctly detected, but other kinds of wheat are misjudged as spotted kernels in varying degrees, resulting in the lowest precision; For the actual 148 sprouted kernels, 137 kernels are correctly detected, 8 sprouted kernels are bulged in the embryo and misjudged as sound kernels, but the predicted sprouted kernels reach 141 kernels, resulting in precision value greater than recall value.

In the results based on Res24\_D\_CBAM\_Atrous, the softmax is used to change the pixel value of the output feature map into a probability distribution, and the maximum probability value is indexed as the prediction probability of the wheat kernel. Finally, the predicted types and probabilities of 6 kinds of wheat kernels are written into the image, and 4 images of each kind of wheat are displayed. As shown in Fig. 9.

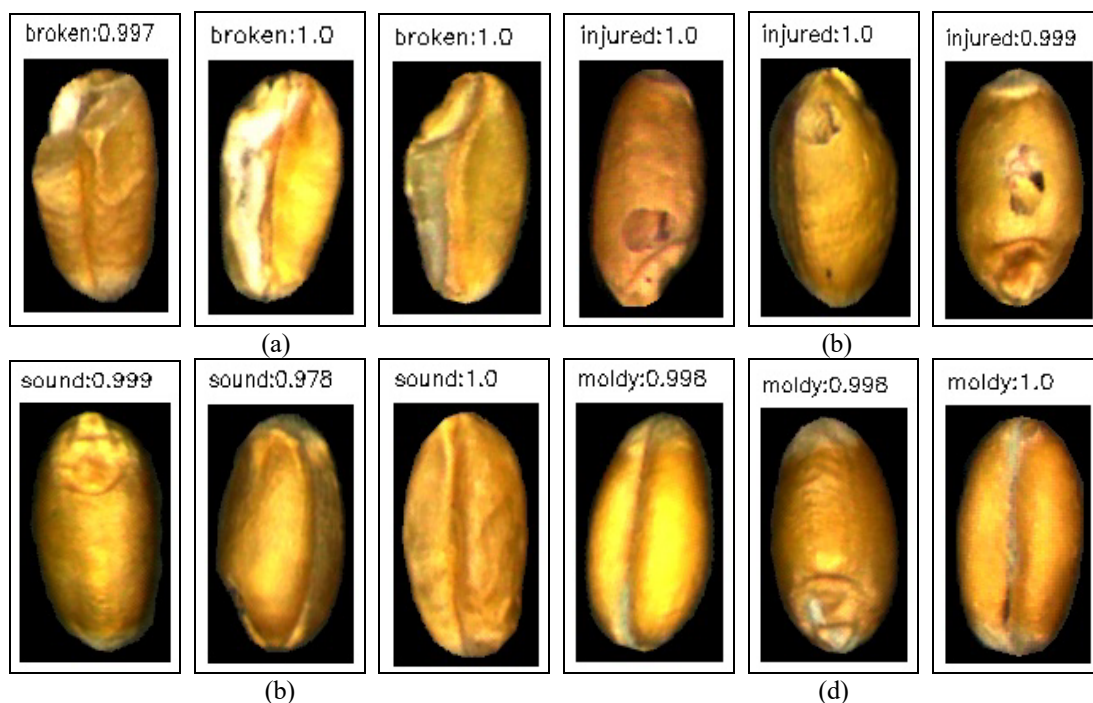






FIGURE 9. Types and probabilities of wheat prediction: (a) broken kernel; (b) injured kernel; (c) sound kernel; (d) moldy kernel; (e) spotted kernel; (f) sprouted kernel

Comparing Res24\_D\_CBAM\_Atrous model with advanced models in this field, the results are shown in Table 4.

TABLE 4. Classification performance evaluation of different models

Paper	Model	Size	Accuracy	Precision	Recall	F1
Zhang et al	ResNet50+CBAM	224×224	0.88	0.88	0.88	0.88
Huang et al	GoogLeNet	224×224	0.85	0.84	0.87	0.85
Altuntas et al	VGG19	224×224	0.81	0.80	0.84	0.81
Kiratiratanapruk et al	InceptionResNetV2	299×299	0.91	0.90	0.93	0.91
Zhu et al	AlexNet	224×224	0.85	0.84	0.86	0.85
Our method	Res24_D_CBAM_Atrous	224×224	0.94	0.94	0.95	0.94

## V. CONCLUSION

In the acquisition and market circulation of wheat, it is a general trend to use computer vision method to detect wheat unsound kernels, but this method is still in the experimental stage. The main reason is that it is difficult to solve the problem of adhesion segmentation of wheat unsound kernels, and the use of equipment alone to realize single kernel of wheat increases the cost and has many difficulties. Some scholars even separate equipment from algorithm, and put wheat in order for identification. In view of the above situation, an image acquisition platform of wheat unsound kernel is built, and the wheat kernels are separated as more as possible by means of vibration. Then, combined with the segmentation algorithm of adhesion wheat with two-kernels based on concave-mask, the concave position is determined by the defect area formed between the adhesive kernels, and the marking segmentation is carried out. By combining the equipment and algorithm, the segmentation error rate is 0.93% in a total of 9988 wheat kernels, which meets the recognition requirements.

In this paper, there are 15360 training sets, 3840 verification sets and 1113 test sets of wheat images. Based on the simple classification model of wheat unsound kernels recognition, by comparing the advantages of GoogleNet, ResNet, DenseNet, ShuffleNet, IX-ResNet, Res2Net, combined with the simple characteristics of wheat unsound kernel, it is found that the depth, width, downsampling mode, attention mechanism, convolution mode and receptive field

size of the model are closely related to the accuracy and prediction speed. The Res34 generates too many similar feature in dimension upgrading, resulting in redundancy. The improved Res24 not only reduces redundancy and computation, but also slightly improves classification performance. The introduction of dense connections in Res24\_D increases the width of the network and enables the model to make full use of the shallow features. The reason why dense connections are not introduced in layer 4 is that too many dense connections will lead to network redundancy. In BN, Relu and Conv, the BN is carried out firstly, which can also reduce the amount of algorithm calculation. The average pooling with  $3 \times 3$  convolution and step of 2 can reduce the loss of characteristic information in the down sampling. The classification of wheat unsound kernel is based on small features such as holes and sprouts. The introduction of attention mechanism in Res24\_D\_CBAM can effectively enhance the ability of feature extraction. The atrous convolution and  $14 \times 14$  feature output introduced in Res24\_D\_CBAM\_Atrous increase the feature receptive field, which makes the model efficiency reach the best. In addition, compared with the advanced models in this field, our model is significantly superior in various evaluation indexes.

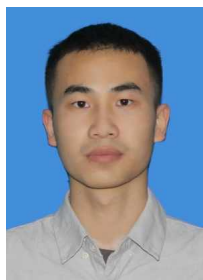
Obviously, the method proposed in this paper can realize the detection of wheat unsound kernels completely and efficiently, which has practical application value, but it still faces many difficulties when it is really applied to the market. There are mainly: the automation level of testing equipment needs to be improved from feeding, segmentation,

classification, calculation and unloading, and it must be combined with multi-view image acquisition to improve the recognition accuracy; The image acquisition scene should be strictly fixed, and a larger unsound kernel data set should be constructed to improve the standardization level; In-depth combination of traditional segmentation, semantic segmentation, instance segmentation to segment more complex adhesion situations; On the basis of classification, the detection standard of unsound kernel rate of wheat based on mass ratio should be established, which provides scientific basis for classification and grading of wheat.

## REFERENCES

- [1] S. Sun, X.G. Yang, X.M. Lin, G.F. Sassenrath, and K.N. Li, "Winter Wheat Yield Gaps and Patterns in China," *Agronomy Journal*. vol. 110, no. 1, pp. 319-330, Jan. 2018.
- [2] C.B. Singh, D.S. Jayas, J. Paliwal, and N.D.G. White, "Detection of insect-damaged wheat kernels using near-infrared hyperspectral imaging," *Journal of Stored Products Research*. vol. 45, no. 3, pp. 151-158, Jul. 2009.
- [3] J.G.A. Barbedo, E.M. Guarienti, and C.S. Tibola, "Detection of sprout damage in wheat kernels using NIR hyperspectral imaging," *Biosystems Engineering*. vol. 175, pp. 124-132, Nov. 2018.
- [4] S. Liu, X. Tan, C.Y. Liu, C.L. Zhu, and W.H. Li, "Recognition of Fusarium Head Blight Wheat Grain Based on Hyperspectral Data Processing Algorithm," *Spectroscopy and Spectral Analysis*. vol. 39, no.11, pp. 3540-3546, Nov. 2019.
- [5] M. Masiello, S. Somma, A. Susca, V. Ghionna, A.F. Logrieco, and M. Franzoni, "Molecular Identification and Mycotoxin Production by Alternaria Species Occurring on Durum Wheat. Showing Black Point Symptoms," *Toxins*. vol. 12, no. 4, pp. 275, Apr. 2020. DOI:10.3390/toxins12040275.
- [6] F.N. Chen, and F. Cheng, "Defective kernel detection using a linear colour CCD," *Imaging Science Journal*. vol. 61, no. 4, pp. 361-368, May. 2013.
- [7] F.N. Chen, P.L. Chen, K. Fan, and F. Cheng, "Hyperspectral Reflectance Imaging for Detecting Typical Defects of Durum Kernel Surface," *Intelligent Automation and Soft Computing*. vol.24, no. 2,pp. 351-357, Jun. 2018.
- [8] H. Liu, Y.Q. Wang, X.M. Wang, D. An, and Y.G. Wei, "Study on Detection Method of Wheat Unsound Kernel Based on Near-Infrared Hyperspectral Imaging Technology," *Spectroscopy and Spectral Analysis*. vol. 39, no. 1, pp. 223-229, Jan. 2019.
- [9] R. Choudhary, S. Mahesh, J. Paliwal, and D.S. Jayas, "Identification of wheat classes using wavelet features from near infrared hyperspectral images of bulk samples," *Biosystems Engineering*. vol. 102, no.2, pp. 115-127, Feb. 2009.
- [10] L. Feng, S. Zhu, F. Liu, Y. He, and C. Zhang, "Hyperspectral imaging for seed quality and safety inspection: a review," *Plant Methods*. vol. 15, no. 1, pp. 91, Aug. 2019.
- [11] M. Guo, Y.T. Ma, X.J. Yang, and R.W. Mankin, "Detection of damaged wheat kernels using an impact acoustic signal processing technique based on Gaussian modelling and an improved extreme learning machine algorithm," *Biosystems Engineering*. vol. 184, pp. 37-44, Aug. 2019.
- [12] A. Suresh, and S. Neethirajan, "Real-time 3D visualization and quantitative analysis of internal structure of wheat kernels," *Journal of Cereal Science*. vol. 63, pp. 81-87, May. 2015.
- [13] M. Koklu, and I.A. Ozkan, "Multiclass classification of dry beans using computer vision and machine learning techniques," *Computers and Electronics in Agriculture*. vol. 174, pp. 105507. Jul. 2020. DOI: 10.1016/j.compag.2020.105507
- [14] S. Javanmardi, S.H.M. Ashtiani, F.J. Verbeek, A. Martynenko, "Computer-vision classification of corn seed varieties using deep convolutional neural network," *Journal of Stored Products Research*. vol. 92, pp. 101800, May. 2021.
- [15] S. Huang, X.F. Fan, L. Sun, and Y.L. Shen, "Research on Classification Method of Maize Seed Defect Based on Machine Vision," *Journal of Sensors*. vol. 2019, pp.1-9, Nov. 2019.
- [16] C. Zhao, L. Quan, H. Li, R. Liu, J. Wang, H. Feng, Q. Wang, and K. Sin, "Precise Selection and Visualization of Maize Kernels Based on Electromagnetic Vibration and Deep Learning," *Transactions of the ASABE*. vol. 63, no. 3, pp. 629-643, 2020.
- [17] C. Ni, D.Y. Wang, R. Vinson, M. Holmes, and Y. Tao, "Automatic inspection machine for maize kernels based on deep convolutional neural networks," *Biosystems Engineering*. vol. 178, pp. 131-144, Feb. 2019.
- [18] Y. Altuntaş, Z. Comert, and A.F. Kocamaz, "Identification of haploid and diploid maize seeds using convolutional neural networks and a transfer learning approach," *Computers and Electronics in Agriculture*. vol. 163, pp. 1-11, Aug. 2019.
- [19] K. Kiratiratanapruk, P. Temniranrat, W. Sinthupinyo, P. Prempree, K. Chaitavon, S. Porntheeraphat, and A. Prasertsak, "Development of Paddy Rice Seed Classification Process using Machine Learning Techniques for Automatic Grading Machine," *Journal of Sensors*. vol. 2020, pp. 1-14, Jul. 2020.
- [20] G. Gilanie, N. Nasir, U.I. Bajwa, and H. Ullah, "RiceNet: Convolutional Neural Networks Based Model to Classify Pakistani Grown Rice Seeds Types," *Multimedia Systems*. vol. 21, no. 5, pp. 867-875, Oct. 2021.
- [21] W.W. Zhang, H.M. Ma, X.H. Li, X.L. Liu, J. Jiao, P.F. Zhang, L.C. Gu, Q. Wang, W.X. Bao, and S.N. Cao, "Imperfect Wheat Grain Recognition Combined with an Attention Mechanism and Residual Network," *Applied Sciences-Basel*. vol. 11, no. 11, pp. 5139, Jun. 2021.
- [22] B. Zhang, "Machine Vision Inseption of Wheat Appearance Quality Based on Deep Learning," Northwest A&F University, ShanXi, China, 2019.
- [23] S.P. Zhu, J.X. Zhuo, H. Huang, and G.L. Li, "Wheat Grain Integrity Image Detection System Based on CNN," *Transactions of the Chinese Society for Agricultural Machinery*. vol. 51, no. 5, pp. 36-42, Mar. 2020. DOI: 0. 6041/j.issn.1000-1298.2020.05.004
- [24] Y.J. Heo, S.J. Kim, D. Kim, K. Lee, and W.K. Chung, "Super-High-Purity Seed Sorter Using Low-Latency Image-Recognition Based on Deep Learning," *IEEE Robotics and Automation Letters*. vol. 3, no. 4, pp. 3035-3042, Oct. 2018.
- [25] Y. Xun, J.X. Zhang, W. Li, and W.G. Cai, "Multi-objective dynamic detection of seeds based on machine vision," *Progress in Natural Science*. vol. 17, no. 2, 217-221, Feb. 2007.
- [26] X.K. Yu, Z.W. Wang, and C.L. Zhang, "Edge Detection of Agricultural Products Based on Morphologically Improved Canny Algorithm," *Mathematical Problems in Engineering*. vol. 2021, pp. 6664970. Jun. 2021. DOI: 10.1155/2021/6664970
- [27] S.Y. Tan, X. Ma, Z.J. Mai, L. Qi, and Y.W. Wang, "Segmentation and counting algorithm for touching hybrid rice grains," *Computers and Electronics in Agriculture*. vol. 162, pp. 493-504, Jul. 2019.
- [28] X.P. Wang, L.J. Yao, H.T. Wen, and J.J. Zhao, "Wolfberry image segmentation based on morphological multiscale reconstruction and concave points matching," *Transactions of the Chinese Society of Agricultural Engineering*. vol. 34, no. 2, pp.212-218, Jan. 2018.
- [29] X. Zhang, C. Zhong, T.H. Huang, and T. Ji, "Method of Image Analysis of Aggregate Particle Group Based on Gray Morphological Reconstruction," *Journal of Building Materials*. vol. 21, no. 6, pp. 886-891, Oct. 2018.
- [30] Z.W. Lyu, H.F. Jin, T. Zhen, F.Y. Sun, and H. Xu, "Small Object Recognition Algorithm of Grain Pests Based on SSD Feature Fusion," *IEEE ACCESS*. vol. 9, pp. 43202-43213, Apr. 2021.
- [31] C. Szegedy, W. Liu, Y.Q. Jia, P. Sermanet, and A. Rabinovich, "Going Deeper with Convolutions," *In proc. IEEE Conf. on Comput. Vis. Pattern Recognit. (CVPR)*, Jun. 2015, pp. 1-9.
- [32] K.M. He, X.Y. Zhang, S.Q. Ren, and J. Sun, "Deep Residual Learning for Image Recognition," *In proc. IEEE Conf. on Comput. Vis. Pattern Recognit. (CVPR)*, Jun. 2016, pp. 770-778.
- [33] H. Gao, Z. Liu, V.D.M. Laurens, and Q.W. Kilian, "Densely Connected Convolutional Networks," *In proc. IEEE Conf. on Comput. Vis. Pattern Recognit. (CVPR)*, Jul. 2017, pp. 2261-2269.

- [34] X.Y. Zhang, X.Y. Zhou, M.X. Lin, and J. Sun, "ShuffleNet: An Extremely Efficient Convolutional Neural Network for Mobile Devices," *In proc. IEEE Conf. on Comput. Vis. Pattern Recognit. (CVPR)*, Jun. 2018, pp. 6848-6856.
- [35] J.S. Park, J.K. Kim, S.H. Jung, and Y.J. Gil, "ECG-Signal Multi-Classification Model Based on Squeeze-and-Excitation Residual Neural Networks," *APPLIED SCIENCES-BASEL*. vol. 10, no. 18, pp. 6495, Sep. 2020. DOI: 10.3390/app10186495.
- [36] J. Miao, S. Xu, and B.Zhou, "ResNet based on feature-inspired gating strategy," *Multimedia Tools and Applications*, Mar. 2021. DOI: 10.1007/s11042-01-10802-6.
- [37] X. Tao, and H. Yang, "IX-ResNet: fragmented multi-scale feature fusion for image classification," *Multimedia Tools and Applications*. vol. 80, no. 18, pp. 27855-27865, Jul. 2021.
- [38] S.H. Gao, M.M. Cheng, K. Zhao, X.Y. Zhang, M.H. Yang, and P. Torr, "Res2Net:A New Multi-scale Backbone Architecture," *IEEE Transactions on Pattern Analysis and Machine Intelligence*. vol. 43, no. 2, pp. 652-662, Feb. 2021.
- [39] Z.Y. Lu, Y.Z. Bai, Y. Chen, C.Q. Su, and S.S. Lu, "The Classification of Gliomas Based on a Pyramid Dilated Convolution ResNet Model," *Pattern Recognition Letters*. vol. 133, no. 5, pp. 173-179, May 2020.
- [40] S.Y. Woo, J.C. Park, and J.Y. Lee, "CBAM:Convolutional Block Attention Module," *In proc. of the European Conf. on Comput. Vision(ECCV)*, Sep. 2018, pp. 3-19.



**HUI GAO** is currently pursuing the master's degree. He majors in computer technology, and his research fields are image processing, deep learning and grain information. He has published two Chinese core journals and accepted one invention patent.



**TONG ZHEN** is a Professor, Doctoral Supervisor, Deputy Secretary General of Information and Automation Branch of Chinese Cereals and Oils Association, and member of Industrial Information Working Committee of China Instrument and Control Society. He has presided over the formulation of 18 national and grain industry standards, compiled 3 books, published more than 100 articles, and more than 30 articles which had been cited by SCI and EI.



**ZHIHUI LI** is an associate professor with doctoral degree. Her research interests are intelligent detection and control, grain information, and she has written many books, and 6 articles have been cited in SCI and EI.